



ELSEVIER

Contents lists available at ScienceDirect

Applied Surface Science

journal homepage: www.elsevier.com/locate/apsusc

Microscopic visualization of cell – Cold sprayed bio-coating interfaces: An intermediate layer formed during the culturing mediates the behaviors of the cells

Yi Liu^{a,b,*}, Wenjia Hou^{a,b}, Rocco Lupoi^c, Shuo Yin^c, Jing Huang^{a,b}, Hua Li^{a,b,*}

^a Key Laboratory of Marine Materials and Related Technologies, Zhejiang Key Laboratory of Marine Materials and Protective Technologies, Ningbo Institute of Materials Technology and Engineering, Chinese Academy of Sciences, Ningbo 315201, China

^b Zhejiang Engineering Research Center for Biomedical Materials, Cixi Institute of Biomedical Engineering, Ningbo Institute of Materials Technology and Engineering, Chinese Academy of Sciences, Ningbo 315201, China

^c Trinity College Dublin, The University of Dublin, Department of Mechanical and Manufacturing Engineering, Parsons Building, Dublin 2, Ireland

ARTICLE INFO

Keywords:

Cell-material interface
Focused ion beam
Cellular behavior
Protein adsorption
Intermediate layer

ABSTRACT

Cold spraying has been proved it is a promising method for biomaterials surface modification and additive manufacturing. Fundamental understanding of the cell-biomaterial interaction is essential for design and fabrication of biomaterials for their biomedical applications. Here we report the evolutionary characteristics of the interfaces between osteoblast cells and cold sprayed hydroxyapatite-titanium composite coating. The *in situ* observation of the interfaces was carried out by focused ion beam-scanning electron microscopy, and influence of the surface characteristics of the coatings on the behaviors of protein adsorption and cell proliferation was examined. Apparent cellular sensing, adhesion, migration, and mineral dissolution after 3 h incubation of the cells were visualized. The predominant existence of fragment particles in the coatings, one of the exceptional features of cold sprayed coating, plays vital role in regulating the cell association and cellular uptake. The presence of Ti and HA fragments at the cell-coating interface had no significant effect on cell viability and cell proliferation. After 5 days culturing, *in vitro* cell fusion and mineralization with the formation of an intermediate layer were evidenced on the coating, suggesting rapid regeneration and accelerated establishment of bone-implant integration. These critical phenomena occurred at different periods of culturing would facilitate understanding the influence of specific surface features of biomaterials on cell responses, and shed light on the development of manufacturing techniques for biomaterials.

1. Introduction

Osseointegration of any orthopedic arthroplasty or dental implant is permanent fixation to the surrounding tissue [1]. The dynamic interfaces between biosystem and biomaterial surfaces regulate cellular adherence, spreading, proliferation and differentiation process of osteoprogenitor cells and ultimately the success of medical implants [2,3]. In this regard, comprehensive understanding of the cell responses on artificial implants is essential for facilitating design and construction of desirable topographical morphology of biomaterials for regenerative tissue engineering. Many techniques were developed in past decades for investigating the cell-material interfaces. Transmission electron

microscope [4,5], scanning electronic microscopy [5,6] and histomorphometric analysis [7,8] are commonly used approaches for visualized characterization of cell-material interface. It is virtually known that upon transplantation of foreign materials into the human body, absorption of key serum proteins on their surfaces takes place as the initial event participating in cell-biomaterial interactions [9]. This is followed by recognition of integrin-mediated cell binding motifs on these proteins, which can in turn regulate signal transduction and important cell processes [2,9,10]. The surface properties have been identified as main determinants of cell fate and tissue integration [2,11,12]. In order to improve the biocompatibility, cell-material interaction can be governed by modification of the surface properties.

* Corresponding authors at: Key Laboratory of Marine Materials and Related Technologies, Zhejiang Key Laboratory of Marine Materials and Protective Technologies, Ningbo Institute of Materials Technology and Engineering, Chinese Academy of Sciences, Ningbo 315201, China. Zhejiang Engineering Research Center for Biomedical Materials, Cixi Institute of Biomedical Engineering, Ningbo Institute of Materials Technology and Engineering, Chinese Academy of Sciences, Ningbo 315201, China.

E-mail addresses: liyui@nimte.ac.cn (Y. Liu), lihua@nimte.ac.cn (H. Li).

<https://doi.org/10.1016/j.apsusc.2020.147132>

Received 5 May 2020; Received in revised form 29 June 2020; Accepted 30 June 2020

Available online 07 July 2020

0169-4332/ © 2020 Elsevier B.V. All rights reserved.

Hydroxyapatite (HA) is the most common calcium phosphate ceramic and is a particularly suitable bone graft substitute owing to its similarity in chemistry to the mineral nature of cortical bone [1,13–15]. For biomedical materials, it has been extensively reported that nanostructures offer the potential for significant improvements in both mechanical strength and biological properties as compared to conventional microphase structures [15–18]. Additionally, nanomaterials also better mimic physiological structures as most tissues *in vivo* have nanoscale features because they are assembled from nanoscale units of amino acids, proteins, and lipids, all of which are in the low end of the nanoscale range in terms of size [18,19]. In this regard, a major challenge remains for HA pertaining to the design and construction of appropriate nanostructures.

Thermal sprayed HA coating on metallic implant for dentistry and orthopedics provides a state-of-the-art template for rapid fixation and strong bonding between the host bone and the implant [1,15,20,21]. However, the intrinsic high temperature accompanied with the coating processing usually leads to certain degree of dihydroxylation, decomposition and grain growth of the starting powder materials [1,22,23]. Cold spray (CS) is known for its ability to deposit advanced 2D/3D materials onto a diversity of substrates with minimum thermal penalty [24–27]. These are the cornerstones that will direct application areas and opportunities lying ahead for CS technique. Yet, the low deposition efficiency, inadequate mechanical properties and poor bonding strength between HA coating and substrate hinder its application for hard-tissue replacement. The limited deformation ability of pure ceramic is a major hurdle that impedes its deposition efficiency via CS processing [24].

To tackle the above mentioned challenges, new approaches to make desired HA coatings are to be explored. Among the measures that have been taken, addition of second phase has been stimulating in promoting deposition efficiency and reinforcing the coating properties [8,26,28–30]. Microstructured HA coatings were deposited by cold spray on PEEK substrate, and enhanced *in vitro* biocompatibility and *in vivo* osteointegration were achieved [8]. HA coated magnesium-based biodegradable alloy via cold spray showed excellent biodegradable and bioactive performances [30]. Our previous finding implied that cold spray is of particular perspective for its outstanding advantages of making nanostructured HA-based coatings for biomedical applications [26]. Generally, during cold spray processing, the tamping effect attained by successive impact of agglomerated particles is essential for consolidating ceramic coatings [31,32]. The previously deposited layers are impacted by subsequent particles which make the former layer considerably denser due to in-situ tamping effect. Utilizing plastic deformation ability of dense metal particles, it is effective to improve the deposition efficiency and mechanical strength of ceramic phase. It is therefore anticipated that the possible tamping of metallic particles applied onto ceramic particles would facilitate densification of the ceramic coatings. In the case of cold sprayed HA coating, the tamping effect could be realized by adding biocompatible metal particles in the starting feedstock powder. Titanium (Ti) and its alloys have been widely used as additive manufacturing materials and medical implant materials due to their excellent mechanical properties and biocompatibility. To construct nano-HA coatings from nano particles, agglomeration by spray-drying processing of the particles was conducted. We used cold spraying technology and the addition of second phase metal particles to resolve nano-grain growth at high temperature and low deposition efficiency of ceramic phase.

For biomedical implants, the persisting major concerns are biocompatibility and structure compatibility. The material-cell interaction is a key determinant for subsequent biological activities after implantation of the materials in human body. The interaction regulates protein adhesion, cellular attachment, motility, adhesion, spreading, proliferation and decides the final fate of artificial implants [2,11]. An important topic in tissue engineering is the effect of topography on cell response, since surface features of biomaterials are signal emitters of cellular behaviors. It has a significant impact on the organization and

type of focal adhesions formed, either by disrupting their formation or by inducing specific integrin recruitment [2]. For cold sprayed bio-ceramic-based coatings, to date, the question of how cold sprayed particles affect the cell behaviors remains largely unexplored. Knowledge on *in vitro* and *in vivo* behaviors of the constructed coatings at different levels, namely animal, organ, cell, sub-cell and molecular, etc., is yet insufficient.

For biomedical coatings, understanding their biological performances is essential for their potential biomedical applications. To understand how cells respond to cold sprayed nanostructure, it is of critical importance to in-situ visualize the cell-coating interaction at different stages. Currently, a combination of *in situ* site-specific focused ion beam (FIB) milling and scanning electron microscopy (SEM) imaging using a wide range of magnifications is a promising approach for directly imaging interface events of individual cells and support material underneath them [3,33,34]. In this paper, HA-Ti composite coatings were deposited by cold spray, and their nanostructural features were characterized. The particular topographical structures of the coatings gave rise to an exceptional coatings-cell interaction regime, which would give insight into fabricating biomedical coatings with desired biological performances.

2. Materials and methods

HA powder in nanosizes was synthesized by the wet chemical approach using stoichiometric reaction between $(\text{NH}_4)_2\text{HPO}_4$ (Aladdin 7783–28-0, China), $\text{Ca}(\text{NO}_3)_2$ (Aladdin C100074, China), and $\text{NH}_3\cdot\text{H}_2\text{O}$ (Aladdin 1336–21-6, China). The spray-drying method was used to produce micro-nanostructured HA beads. Nanosized HA powder was mixed with 2 wt% poly(vinyl alcohol) (PVA, Aladdin 9002–89-5, China) binder in water with the concentration of 50 g/L. Dispersed HA suspension was injected into a chamber of spray-drying equipment (LPG, Changzhou Xingyu Drying Equipment Co., Ltd, China). The inlet air temperature was 210 °C with the rotary speed of 190 r/s and the liquid feed rate was 30 mL/min. The HA beads were then sintered at 900 °C for 2 hrs to remove the PVA binder and to consolidate the beads. Kinetiks-4000 cold gas spray system (CGT Cold Gas Technology GmbH, Ampfing, Germany) with Kinetiks PF4000 powder feeders were utilized for the spraying. Nitrogen was used as the accelerating gas and powder carrier gas. The agglomerate nanostructured HA powder with an average size of 40 μm (Fig. 1a) was mechanically mixed with titanium powder ($d_{0.5} = 50 \mu\text{m}$, TLS Technik GmbH, Germany) and then cold sprayed onto $\text{Ti}_6\text{Al}_4\text{V}$ substrates operated at 500 °C with the gas pressure of 3.5 MPa. The standoff distance was 20 mm and gun traverse speed was 40 mm/s.

Microstructure of the coatings was characterized by field emission scanning electron microscopy (FESEM, FEI Quanta FEG250, the Netherlands) and laser confocal microscope (ZEISS, LSM700, Germany). The function of Z-stack 3D imaging was used to measure the surface morphology of CS coating. Scanning speed is 2 frames/sec with 512×512 pixels. Precision of sample positioning is guaranteed by piezoelectric linear motors with minimum x and y step size 10 nm. The scanning distance of each layer is 20 nm along the height direction (Y axis). And, it was used to measure surface roughness R_a parameters.

Adsorption of serum proteins on the surfaces of the coatings was analyzed using the bicinchoninic acid (BCA) protein assay. The $\text{Ti}_6\text{Al}_4\text{V}$ plates and HA-Ti coatings were immersed in 3 key serum protein solution (1 mg/mL albumin, 0.3 mg/mL fibronectin and 0.3 mg/mL vitronectin) for 1 h, respectively. Subsequently the samples were rinsed with PBS to remove unadsorbed protein molecules and shaken in 1 mL 1% SDS for 1 h. After adding BCA working reagent (1.0 mL), each sample was incubated at 37 °C for 30 min. The amount of adsorbed protein was measured by optical density (OD) at 562 nm using SpectraMax 190 Microplate Reader (Molecular Devices, USA).

Cell culture experiments were conducted using the human osteoblast cells (HFOB 1.19 SV40 transfected osteoblasts) using α -minimum

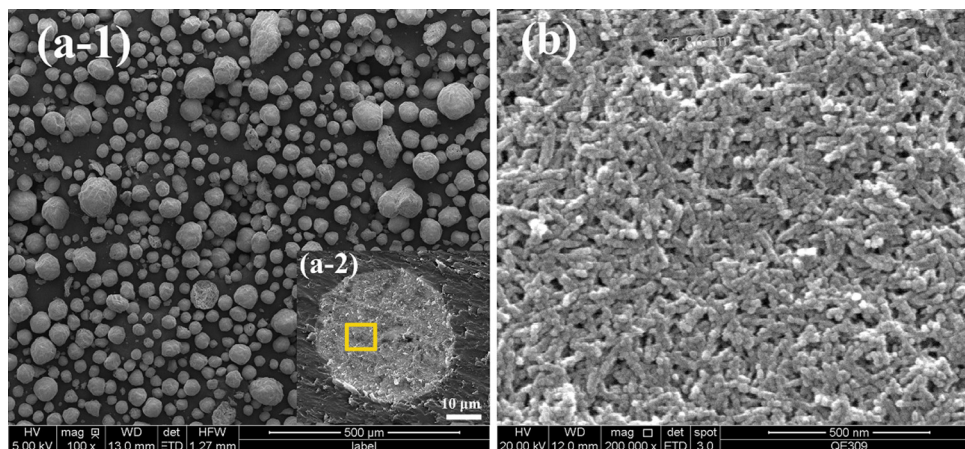


Fig. 1. (a-1) Typical morphology of the starting nSD-HA particles and the inset (a-2) shows cross-section of HA microsphere. Magnified view of the typically selected area from (a-2) shows the agglomeration of nanosized HA powders (b).

essential medium (α -MEM, SH30265.01B, HyClone, USA) supplemented with 10% heat-inactivated fetal bovine serum in an atmosphere of 100% humidity and 5% CO_2 at 37 °C. For the testing, the cells were seeded at a density of 2000 cells/ cm^2 onto the samples in 24-well plates with 2 mL media containing 10% heat-inactivated fetal bovine serum in each well and grew under standard culture conditions for 3 hrs, 1 d, 3 d and 5 d. Prior to seeding, the samples were autoclave sterilized for 30 min. Proliferation and biocompatibility of the HA-Ti coatings were examined by MTT assay. The human osteoblast cells were cultured on tissue culture polystyrene (TCPS)-24 well plates as control. Paired student's *t*-distribution was employed to clarify the level of significance (*p*) in difference between two sets of data. Data was presented with standard deviation (\pm SD) and statistical significance was set at $p < 0.05$ as determined by the Student's *t*-test. The adhesion and spreading of cells and the cell-coating interfaces were observed by FIB/SEM system (Carl Zeiss Auriga, Germany). For in-situ observation of the adherent cells on the coatings surfaces, the proliferated cells were fixed in 2.5% glutaraldehyde for 24 hrs, dehydrated gradually and coated with Au. Prior to Ga^+ milling and polishing, the protective platinum strip (\sim 500 nm thick) was deposited on the cells.

Sample labels: Hydroxyapatite (HA); Spray-dried HA (nSD-HA); Titanium (Ti); Cold spray (CS); Hydroxyapatite-titanium composite coating (HA-Ti coating); Cold sprayed hydroxyapatite-titanium composite coating (CS HA-Ti coating); $\text{Ti}_6\text{Al}_4\text{V}$ substrate ($\text{Ti}_6\text{Al}_4\text{V}$);

3. Results and discussion

The spray-dried HA (nSD-HA) feedstock particles exhibit the sizes of 25–100 μm in diameter (Fig. 1 a-1) and dense structure (inset in Fig. 1 a-2). HA microsphere is formed by the agglomeration of individual rod-shaped nanosized HA powders. Close examination of cross-sectional part of the spherical individual particles shows the nanostructures with rod-like powders with the size of \sim 120 nm in length and \sim 50 nm in diameter (Fig. 1 b).

HA-50wt.%Ti coatings fabricated by cold spraying show a uniform thickness and a tightly adhered structure to $\text{Ti}_6\text{Al}_4\text{V}$ substrate (Fig. 2 a). Adiabatic shear instability has been acknowledged as one of the dominant mechanisms during cold spraying [24,35,36]. The Ti particles undergo severe plastic deformation as they impact at high velocity on the substrate. Besides promoting the increment in bonding strength, the shear stress and plastic deformation of the Ti particles may facilitate HA deposition [28,29]. Yet surprisingly, the nSD-HA particles are crushed into small pieces and partially embedded in surrounding Ti during the coating formation. HA phase being a ceramic lacks deformability that is a key requirement for cold spray. The hard/soft mixture powders were created by mechanical dispersion of ceramic/metallic particles. The as-

sprayed coatings are deposited with nano-sized HA particles embedding in a softer Ti matrix. Consequently, some HA particles are retained by being embedded in the deformed Ti spread particles whereas some are nicely compacted between the Ti particles. Surface topography of the coatings was captured in FIB machine with the specimen being tilted for 52°. Typical rough morphology is seen on the top surface (Fig. 2 b), which might act as anchor points, in turn facilitating adsorption of cell surface proteins. This was further justified by the 3D image analysis (Fig. 2 d) and cell response testing (Fig. 4).

Based on these observations, the tamping and in-situ shot peening effects of Ti particles is suggested, which are effective to improve the densification of nanostructured HA coatings [37]. In this case, loose structures of previously deposited HA can be removed by erosion effect. Meanwhile, creation of the residual craters is a result of the shot rebounding of the impacting particles occurred as their velocity is lower than the critical value (Fig. 2 c and d). Generally, auxiliary continuous tamping, squeeze, shear and blast of metallic particles is necessary for ceramic coatings consolidation, and dense microstructure and crater-island-shaped morphology is the typical topographical feature. For the cold sprayed HA-Ti coatings, their structural features further evidenced the tamping effect brought about by the Ti particles during the spraying.

It is established that attachment, immigration and proliferation of osteoblast cells are sensitive to the surface texture of biomaterial in early stage of tissue-biomaterial interaction for bone regeneration. Surface roughness is one of the critical parameters that affect cell-biomaterial interactions. Further examination of the topographical morphology by laser confocal microscope provides roughness parameters as well as three-dimensional views of the coatings at their surfaces (Fig. 2 d). The arithmetic mean roughness R_a shows an average value of approximately 13.4 μm . The diameters of the “craters” range from 15 to 50 μm with maximum depth of \sim 40 μm . Accordingly, the vertical height of the “islands” is 10–40 μm (Fig. 2 d).

It is virtually known that upon contact of cells or tissues with biomaterial, initial absorption of serum proteins from biological fluids on the material surface takes place as the initial event participating in the material-cell interactions. There are more than 150 proteins known in human blood serum. Among the important proteins in human blood serum, fibronectin (Fn) [38] and vitronectin (Vn) are obligate adhesive ones for integrin-receptor-based adhesion and spreading of cells on material surfaces [2,38,39]. Human serum albumin (HSA) is the most abundant protein in blood plasma and is evidenced to eliminate cell attachment and block nonspecific binding [40]. In this study, Fn, Vn and HSA were chosen as typical molecules to examine at molecular level the biological significance of the physiochemical characteristics of the cold sprayed HA-Ti coatings.

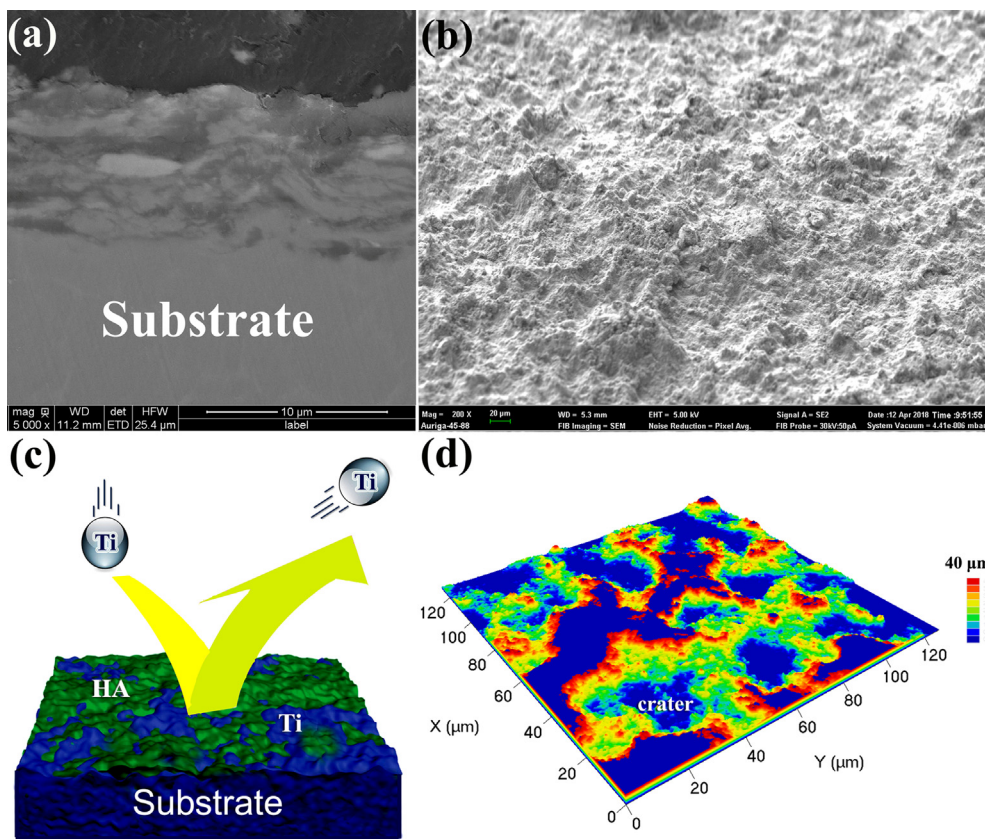


Fig. 2. (a) Typical cross-sectional view of the HA-Ti coating cold sprayed on Ti6Al4V substrate. (b) Tilted FESEM view (52°) of the HA-Ti coating surface. (c) Schematic illustration showing tamping and in-situ shot peening effects attained by Ti particles that promoted ceramic coatings consolidation and formation of the HA-Ti coating. (d) laser confocal microscopy observation of the as-deposited coatings.

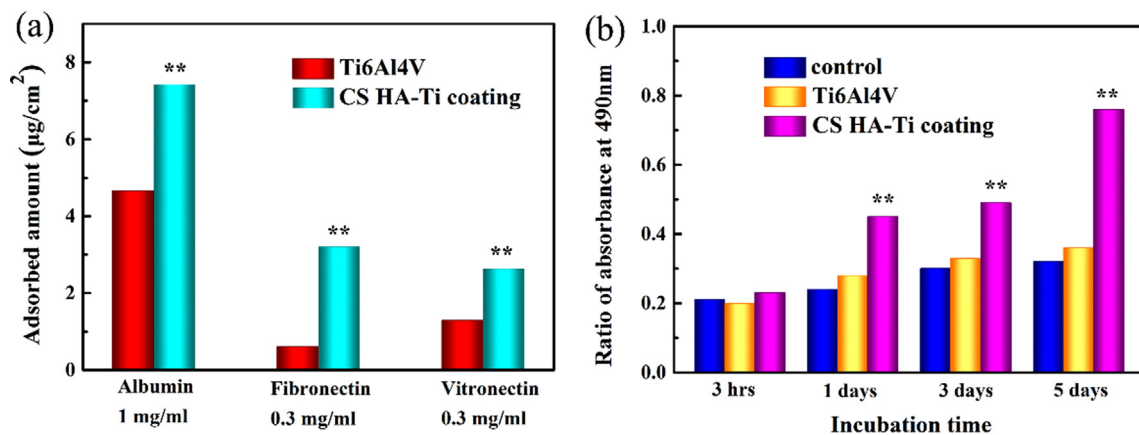


Fig. 3. (a) Adsorption of serum proteins and (b) cell culture results for the HA-Ti coatings. The proteins (albumin, fibronectin, vitronectin) and osteoblast cells cultured on the coated surfaces show enhanced adsorption/proliferation behaviors. **p < 0.05 as compared with the Ti₆Al₄V substrate (analyzed by paired Student's t-test).

In this case, the adsorbed proteins are in good agreement with the cells attached/proliferated on the surfaces of the samples (Fig. 3). The micro-nano-scaled surface texture improved the adhesive molecular interaction with the HA-Ti coatings (Fig. 3 a), giving in part rise to the enhanced cellular attachment and proliferation (Fig. 3 b). The early adsorption of albumin, fibronectin and vitronectin presumably suggests that surface features promote the extracellular matrix (ECM) formation, which in turn facilitates cell culture. The original HA phase and the nanosize of the grains are completely retained after the coating deposition [26,28,29], biological performance of medical titanium alloy can be significantly improved via surface functional modification of cold spraying. Additionally, high surface roughness might play roles in regulating cell-material interaction through influencing adsorption of key serum proteins, rougher substratum with “craters” and “islands”

bound higher amount of total proteins and adhesive proteins than the smoother Ti₆Al₄V substrate (Fig. 3 a).

The topographical features of the coatings take part in coating-cell interaction. Results show that the coatings favor the attachment of the cells on their surfaces. The cells exhibit faster spreading and better stretching state on the HA-based coatings than on Ti alloy, as well as greater cell spreading and adhesion on craters than on islands (Fig. 4 a). Interestingly, as noticed from the close view of the cells grown on the coating surface, the filopodia of the cells incline to exhibit a hole-filling state and bridge over the craters (Fig. 4 a). Since the micro-sized craters possess relatively high storage capacity for biological fluids especially biomolecules, which might favor adsorption of serum proteins for integrin-receptor-based cell adhesion and spreading on the crater-rich areas. Accordingly, cells opt to grow around the areas and gradually

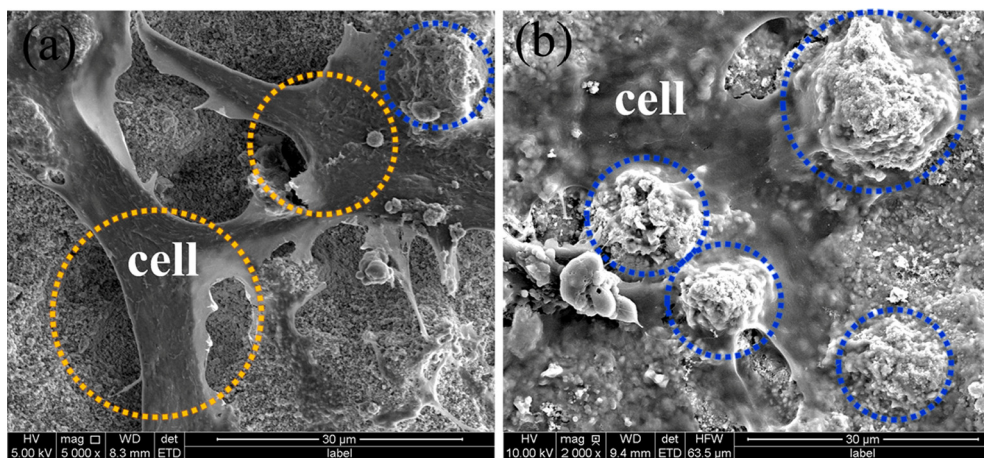


Fig. 4. Cell culture results for the HA-Ti coating surface. (a) The craters are marked by yellow circles, while the islands areas are enveloped by the blue circles (b). The cells incline to cover the craters rather than the islands. (For interpretation of the references to colour in this figure legend, the reader is referred to the web version of this article.)

spread over the islands (Fig. 4 b and Fig. 8), for this surface texture is sensed as barriers. Pioneering work already proposed a generalized cell response to changes in island size, implying islands height of greater than 40 nm decreased cell adhesion [2,41]. This phenomenon suggests a special assembly style of cells growing on the cold sprayed coating in a well-defined geometry.

Understanding of tissue-biomaterial interaction is essential for designing and construction of desired surfaces of the biomaterials. Evolution of the interfaces between the HA-Ti coatings and the cells during the cell culturing testing was visualized via SEM on a transverse section conducted by FIB milling. This approach can be used to observe and record detailed information about important cellular responses that are primarily involved in cell-material interactions.

After culturing after 3 h, cellular sensing, adhesion, migration, and mineral dissolution were realized underlying the partially spreading cells. Notably, the cell probes surrounding environment and moves using their filopodias (Fig. 5b-1 and b-2). Since their receptors and filopodias at cellular membrane are structured at nanoscale level of 80–200 nm (Fig. 5 b-2), cells are likely to rapidly respond to the composite nanostructures in order to find suitable sites for adhesion and growth. Moreover, the ends of filopodias serve as anchor points for migration and adhesion [19,42]. Furthermore, integrin receptors bind

absorbed proteins (e.g. fibronectin, vitronectin) on coating surface, in turn forming the focal adhesions (FAs) as indicated by red arrows shown in Fig. 5 b-2 and b-3. The jet of individual Ti particles and accumulation of HA particles in the first layer of the coating are also clearly visualized. It is noted that cells are able to establish FAs with interfacial jet and HA particles (Fig. 5 b-2), enabling an intimate contact and hence facilitating cell-coating bonding (Fig. 5 b-1). The cellular response, particularly cell attachment, could be explained by the promoted adsorption of the key serum proteins on the retained HA nano-grains. Yet, interestingly, the partially dissolved regions appear to be localized in the residual pores adjacent to the HA-rich areas, which are preferentially distributed across the coating surface, indicating degradation that initiates from HA fragments after only 3 h incubation (Fig. 5 b-4). This suggests the impact of the slight dissolution of HA on the bioactivity of these coatings.

The primary cell's capacity to proliferate and differentiate is influenced by its attachment, adhesion and spreading at first phase upon contact with biomaterial. For the nanostructured HA-Ti coatings, after 1 day incubation, cell division and proliferation are particularly recognized between the two cells (cell 2 and cell 3, Fig. 6 a-1), giving rise to segregation of two nuclei, simultaneously accompanied with cell segregation (Fig. 6 a-2) or conjunction between cell 1 and cell 3 from

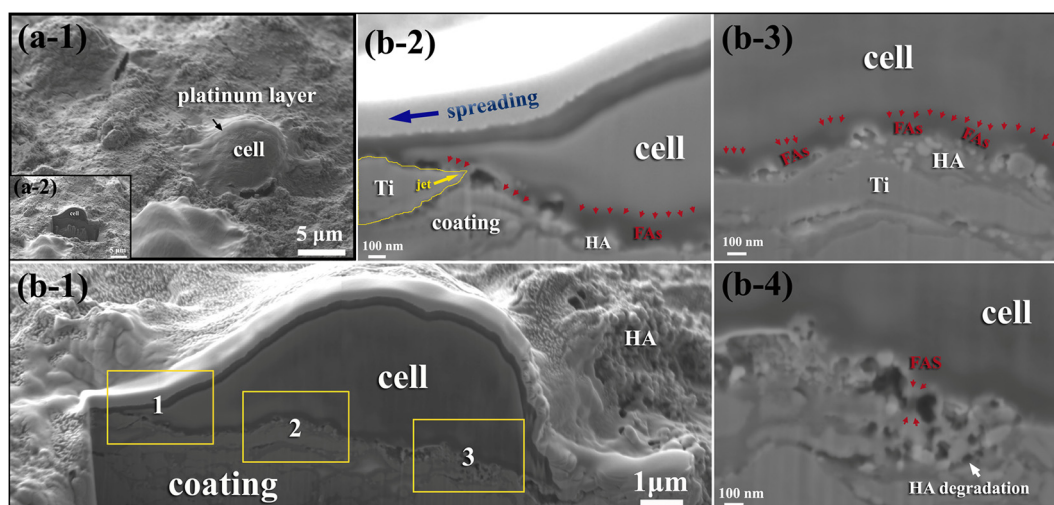


Fig. 5. (a-1) Secondary electron micrographs taken at 52° tilting angle showing individual osteoblast attached on the HA-Ti coating after 3 hrs incubation (the sample was coated with a thin platinum layer). (a-2) The inset shows a panoramic view of adherent cell-coating interface after ion polishing. (b-1) Close view of cellular response to the coating surface. (b-2) The osteoblast filopodia sensing surrounding environment and spreading on the HA-Ti coating. (b-3) The formation of focal adhesions (FAs), and (b-4) partial dissolution of HA grains at cell-coating interface. The red arrows point to focal adhesions (FAs). The image (b-2), (b-3) and (b-4) are magnified views of box 1, box 2 and box 3 highlighted in (b-1), respectively. (For interpretation of the references to colour in this figure legend, the reader is referred to the web version of this article.)

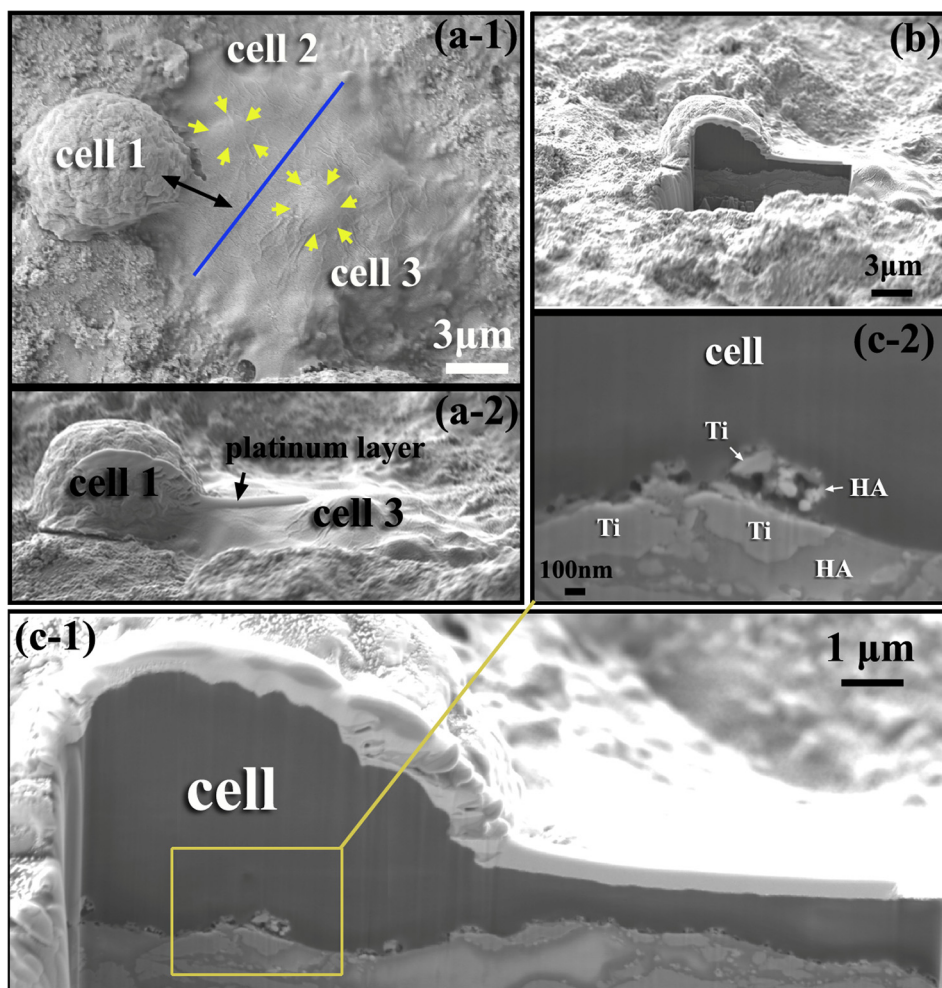


Fig. 6. (a) Secondary electron micrographs showing cell division on the HA-Ti coating after 1 day incubation (-1: vertical view, -2: side view). The dividing nuclei and cytoskeletal rearrangement underlying the plasma membranes are clearly seen. (b) A panoramic view of cell-coating interface showing the region of interest for the sequential ion milling. (c-1) Enlarged cross-sectional view revealing the close contact of the plasma membrane on the HA-Ti coating surface. The yellow box highlights the region with non-specific pinocytosis. (c-2) Uptake of HA and Ti fragments by osteoblast on the HA-Ti coating as revealed by FIB-SEM. (For interpretation of the references to colour in this figure legend, the reader is referred to the web version of this article.)

the cross-sectional views (Fig. 6 b and c-1). Additionally, cytoskeletal re-arrangement underlying the plasma membranes of two neighboring cells takes place during cell replication (Fig. 6 a-1). These phenomena demonstrate that the HA-Ti coatings promote proliferation of the cells attached on their surfaces.

Currently, mechanical interlocking and metallurgical bonding are commonly recognized as the two major adhesion mechanisms for cold sprayed coatings [24,35,36]. Particle-cell association and cellular uptake may influence correlated cytotoxicity and biostability which is a vital issue for biomedical applications [43,44]. Some Ti particles undergo significant fraction and crush into fragments due to high impact strength [45], whereas nSD-HA is broken down to their nanoparticle components. The fragments near the cell surface are more prone to be engulfed. It is noted that cellular uptake of detached Ti fragments of ~200 nm and particulate HA debris of ~50 nm can be observed from the surface of the coating (Fig. 6 c-2), indicating that osteoblasts initially 'swallow' particles near the top coating layer after 1 day incubation, even though the cell might not spread well on the coating surface. The non-specific pinocytosis process originates from the ruffled membrane invagination (Fig. 6 c-2) and the plasma membrane further wraps around the external fragments to form vesicles (Fig. 7). Meanwhile, the micro-sized Ti fragments could not penetrate the cell membrane due to their large size, evidencing the dependence of cellular uptake on debris size.

After culturing for 3 days, leading edges of the cells spread out onto the coating surface and flatten down to ~100 nm (Fig. 7 a-1 and a-2). FIB-SEM characterization further showed that cells engulfed along the particle-cell interface and the fragment clusters penetrated into the

cells. The MTT result and cellular growth morphologies clearly demonstrated that the Ti and HA fragments had no remarkable negative effect on the cell viability and cell proliferation (Fig. 7 b-1 and b-2). Studies have claimed that sphere- and rod-shaped HA nanoparticles induced significantly less cytotoxicity than needle- and plate-shaped ones [46].

Chemistry and structure of biomaterials are the two important variables that determine the rate of degradation and consequently alter or control biomaterial-tissue interactions and bone remodeling. The HA particles that are in intimately contact with the cells are progressively degraded, forming an intermediate layer between cells and the coating (Fig. 7 b-2 and b-3). Generally, HA degradation is initiated accompanied with phagocytosis and followed by intracellular degradation in phagolysosomes, which is one of the main mechanisms of cell-mediated material solubilization [47]. In the absence of osteoblasts and extracellular matrix (ECM), HA nano-grains were loosened and dissolved after culturing periods as short as 3 h (Fig. 5 b-4). After elongated exposure of 3 days, the considerable degradation shows an abundance of small pores (50–200 nm) spreading out across the surface (Fig. 7 b-3). Furthermore, calcium and phosphate ions would be released into the surrounding physiological environment as the calcium phosphate dissolves. Ion exchange and new crystalline apatite is subsequently precipitated from the calcium and phosphate ions in the physiological fluid [21,48,49]. The establishment of an intermediate layer corresponds to the dynamic balancing of degradation and dissolution of bioactive layer [50]. Eventually, degradable phases are partially resorbed and incorporated into remodeled calcium phosphate layer that lead to stronger bonding between cell-coating [21]. Degradation and

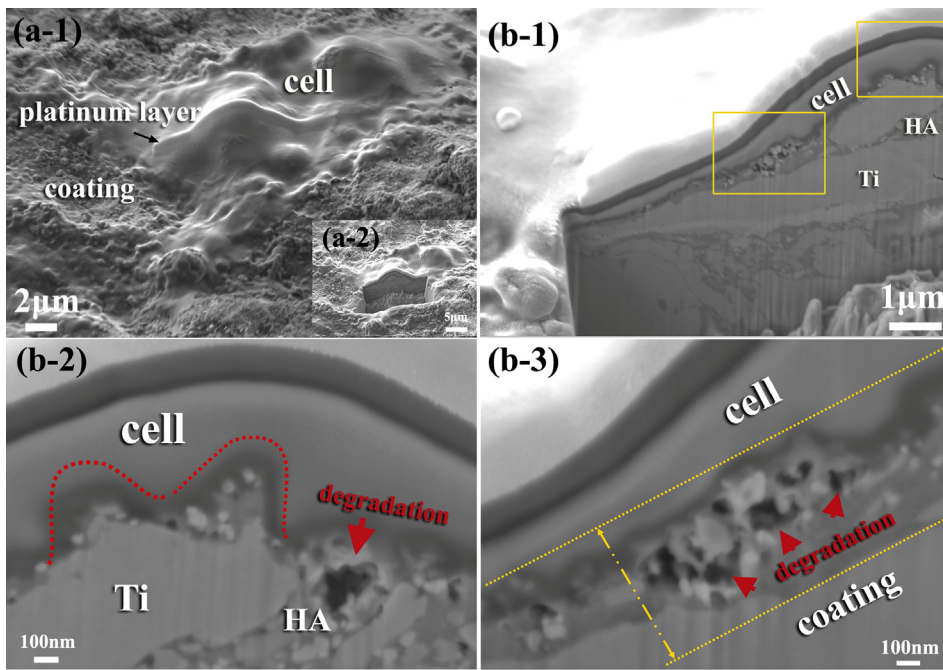


Fig. 7. (a-1) Secondary electron micrographs of the cells spreading on the HA-Ti coating after 3 days incubation. (a-2) The inset shows the SEM micrograph taken at the same location after ion milling. (b) An overview image of the cross section showing the interface between cell and coating. The yellow boxes highlight the regions shown in (b-2) and (b-3). (b-2) The typical cellular uptake and degradation around the coating. The red dotted curves denote the areas for membrane invagination that is extremely prone to form vesicles. The red arrows point to the location where HA degradation occurred. (b-3) The yellow dashed arrow highlights an intermediate layer across the coating surface. (For interpretation of the references to colour in this figure legend, the reader is referred to the web version of this article.)

resorption of the physiological regions create a new extracellular microenvironment owing to different microstructure, chemical composition and ion concentration that further regulate subsequent cellular functions and biological events around the implant.

While after 5 days culturing, osteoblasts present fully flat and the

cellular coverage is up to 95% (Fig. 8 a-1). The cells form a closely packed sheet on the coating surface, indicating the HA-Ti coating possesses outstanding capability for cellular recruitment and organization. Moreover, the coating surface is thoroughly occupied by extensive spreading cell which promotes osteoconduction to bridge large

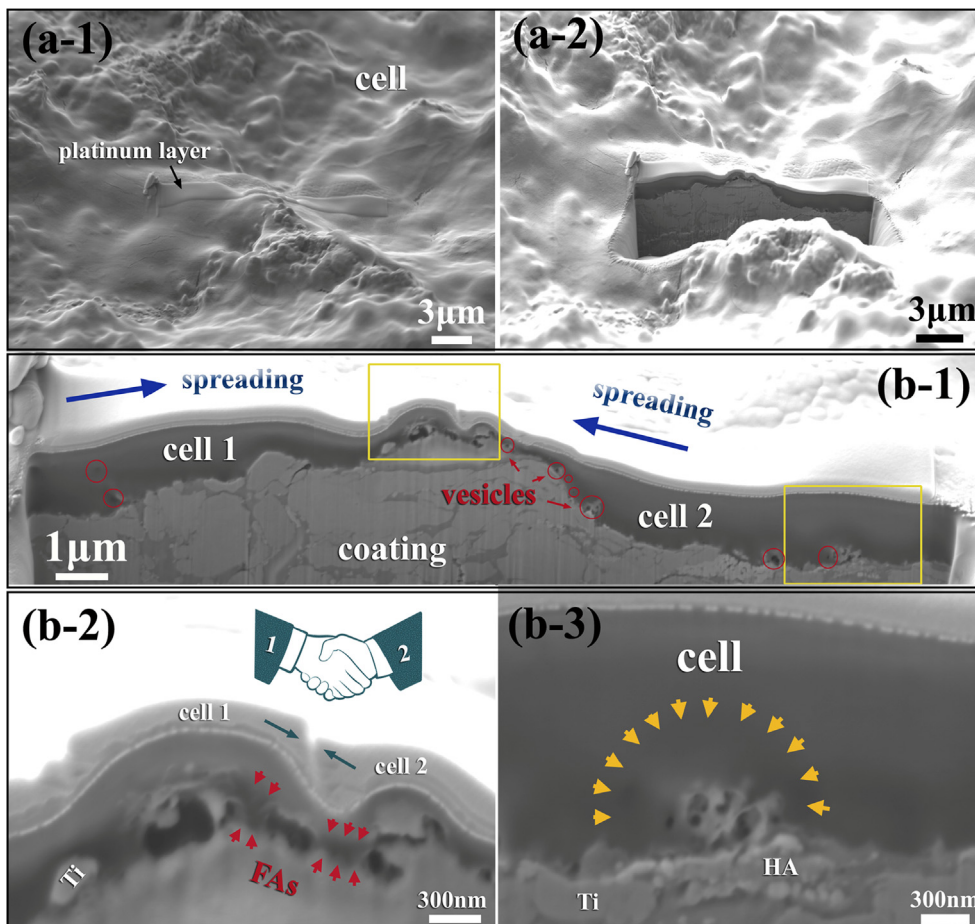


Fig. 8. (a-1) Secondary electron micrographs showing the formation of cell aggregates and masses on the HA-Ti coating after the incubation time of 5 days, and (a-2) corresponding SEM micrograph after ion milling. (b-1) The cross-sectional view showing a strongly confluent layer of osteoblastic cells and cell fusion and accumulation of numerous vesicles. Yellow boxes highlight the regions of (b-2) and (b-3). (b-2) Visualization of intercellular response showing the development of cellular fusion and formation of a continuous cellular sheet. Green arrows point to de-adhesion and interlocking of the cells. (b-3) Mineralization is apparent in close proximity to collagen fibers near cell plasma membrane, suggesting the progressive bone remodeling and new bone formation at the cell-coating interface. Yellow arrows point to the site of newly formed nanocrystal fibers. (For interpretation of the references to colour in this figure legend, the reader is referred to the web version of this article.)

gaps. Actually, bone repair cannot be realized by individual osteoblasts because their *in vitro* differentiation is affected by cell density as well as endogenous and exogenous inhibitors [51]. Integrins are the major transmembrane components existing in FAS, and they also participate in cell–cell communication. The disassembly of FAs and cellular de-adhesion occurred during the transition from flat to round cells, which tightly coordinate with the formation of intercellular junctions (Fig. 8 b-2). These further promote notably the interaction of one cell with another (Fig. 8 b-2) and their aggregation to form interlocked masses and tissue (Fig. 8 a-2 and b-1). The accumulation and fusion of cells is ready to launch subsequent differentiate and mineralization.

Massive numbers of vesicles shed at plasma membrane of osteoblasts and serve as nucleation sites for crystalline apatite precipitation (Fig. 8 b-1 and b-3). These vesicles may have multifunctions, including facilitating cellular communication, causing fragments uptake and extending cell membrane surface to support mineralization [51]. The intracellular calcium signal regulates gene transcription and further triggers vesicles to form HA nanocrystals [52].

The absence of mineralization has been identified as an important feature that improves osseointegration. Further FIB-SEM observation shows newly formed nanocrystal fibers of 50 nm in diameter and 300 nm in length at cell-coating interface, suggesting an initial period of mineralization of collagen fibers (Fig. 8 b-3). Small bone mineral crystals are identified in this area. Osteoblasts are responsible for the bone mineralization during bone remodeling. They secrete type I collagen and matrix organizing proteins that further support crystal nucleation and epitaxial re-precipitation. Moreover, bone cells could retract deposited collagen anchored to a layer of loose HA grains by epitaxially precipitated HA. It is known that bone remodeling is completed by osteoblastic bone formation and mineralization of bone matrix at tissue-implant interface. Biological fixation can be ultimately achieved through the bidirectional growth of a bonding layer, which was visualized in this work.

The results showed that the HA-Ti composite structure could enable rapid regeneration and complete establishment of bone-implant integration, providing a favorable environment for osteoblastic activities. The special surface nanostructures of the cold sprayed HA-Ti coatings can promote early and strong fixation. It is hypothesized that the coatings may accelerate cell-coating integration rate *in vitro* than traditional coatings made by other thermal spray techniques. The FIB-SEM characterization of the cell-biomaterial interfaces would give insight into understanding both the host response and material response, in turn facilitating design and fabrication of biomaterials for desired performances.

4. Conclusions

The dynamic cell - material interaction were characterized by focused ion beam-scanning electron microscopy. After exposing the cells to coating surface, cell uptake of Ti and HA fragments exhibited biostability and nontoxicity. Compared to titanium alloys as gold standard, the micro-nano-scaled surface texture of CS HA-Ti coatings improved the adsorption of fibronectin, vitronectin and albumin, giving rise to the enhanced cell viability in an initial stage of cell-material interaction. Cellular sensing, adhesion and migration is accompanied by mineral dissolution underlying the partially spreaded cells after 3 h of *in vitro* incubation. Bioactive HA-Ti coating could stimulate the rapid development of an intermediate layer after 3 days and further improve tissue regeneration between the implant and surrounding tissues after 5 days. It is anticipated to give certain insights into design and fabrication of bioactive coatings with mediatable cellular behaviors for biomedical applications.

Declaration of Competing Interest

The authors declare that they have no known competing financial interests or personal relationships that could have appeared to influence the work reported in this paper.

Acknowledgements

This research was supported by National Natural Science Foundation of China, China (grant # 31500772), Zhejiang Provincial Natural Science Foundation, China (grant # LY18C100003), The Youth Innovation Promotion Association of the Chinese Academy of Sciences, China (grant # 2020299) and Innovation 2025 Major Special Programme of Ningbo, China.

References

- [1] C. Hu, D. Ashok, D.R. Nisbet, V. Gautam, Bioinspired surface modification of orthopedic implants for bone tissue engineering, *Biomaterials* 219 (2019) 119366.
- [2] K. Anselme, P. Davidson, A.M. Popa, M. Giazzon, M. Liley, L. Ploux, The interaction of cells and bacteria with surfaces structured at the nanometre scale, *Acta Biomater.* 6 (2010) 3824–3846.
- [3] F. Santoro, W. Zhao, L.M. Joubert, L. Duan, J. Schnitker, Y. Burgt, H.Y. Lou, B. Liu, A. Sallou, L. Cui, Y. Cui, B. Cui, Revealing the cell-material interface with nanometer resolution by focused ion beam/scanning electron microscopy, *ACS Nano* 11 (2017) 8320–8328.
- [4] L. Hanson, Z.C. Lin, C. Xie, Y. Cui, B. Cui, Characterization of the cell-nanopillar interface by transmission electron microscopy, *Nano Letter* 12 (2012) 5815–5820.
- [5] C.S. Hansel, M.N. Holme, S. Gopal, M.M. Stevens, Advances in high-resolution microscopy for the study of intracellular interactions with biomaterials, *Biomaterials* 226 (2020) 119406.
- [6] T. Okada, T. Ogura, High-resolution imaging of living mammalian cells bound by nanobeads-connected antibodies in a medium using scanning electron-assisted dielectric microscopy, *Sci. Rep.* 7 (2017) 43025.
- [7] J.H. Lee, H.L. Jang, K.M. Lee, H.R. Baek, K. Jin, K.S. Hong, J.H. Noh, H.K. Lee, *In vitro* and *in vivo* evaluation of the bioactivity of hydroxyapatite-coated poly-etheretherketone biocomposites created by cold spray technology, *Acta Biomater.* 9 (2013) 6177–6187.
- [8] J.H. Lee, H.S. Ryu, D.S. Lee, K.S. Hong, B.S. Chang, C.K. Lee, Biomechanical and histomorphometric study on the bone-screw interface of bioactive ceramic-coated titanium screws, *Biomaterials* 26 (2005) 3249–3257.
- [9] C. González-García, M. Cantini, J. Ballester-Beltrán, G. Altankov, M. Salmerón-Sánchez, The strength of the protein-material interaction determines cell fate, *Acta Biomater.* 77 (2018) 74–84.
- [10] J.H. Wang, B.P. Thampatty, J.S. Lin, H.J. Im, Mechanoregulation of gene expression in fibroblasts, *Gene* 391 (2007) 1–15.
- [11] X. Yao, R. Peng, J. Ding, Cell-material interactions revealed via material techniques of surface patterning, *Adv. Mater.* 25 (2013) 5257–5286.
- [12] S. Bodhak, S. Bose, A. Bandyopadhyay, Role of surface charge and wettability on early stage mineralization and bone cell-materials interactions of polarized hydroxyapatite, *Acta Biomater.* 5 (2009) 2078–2088.
- [13] M.I. Kay, R.A. Young, Crystal structure of hydroxyapatite, *Nature* 204 (1964) 1050–1052.
- [14] A. Szcześ, L. Hołysz, E. Chibowski, Synthesis of hydroxyapatite for biomedical applications, *Adv. Colloid Interface Sci.* 249 (2017) 321–330.
- [15] D. Arcos, M. Vallet-Regí, Substituted hydroxyapatite coatings of bone implants, *J. Mater. Chem. B* 8 (2020) 1781–1800.
- [16] H.J. Zhou, J. Lee, Nanoscale hydroxyapatite particles for bone tissue engineering, *Acta Biomater.* 7 (2011) 2769–2781.
- [17] J. Wang, L.L. Shaw, Nanocrystalline hydroxyapatite with simultaneous enhancements in hardness and toughness, *Biomaterials* 30 (2009) 6565–6572.
- [18] C. Nune, R.D.K. Misra, M.C. Somani, L.P. Karjalainen, Dependence of cellular activity at protein adsorbed biointerfaces with nano- to microscale dimensionality, *J. Biomed. Mater. Res. Part A* 102A (2014) 1663–1676.
- [19] P.K. Mattila, P. Lappalainen, Filopodia: molecular architecture and cellular functions, *Nat. Rev. Mol. Cell Biol.* 9 (2008) 446–454.
- [20] U. Ripamonti, L.C. Roden, L.F. Renton, Osteoinductive hydroxyapatite-coated titanium implants, *Biomaterials* 33 (2012) 3813–3823.
- [21] L. Sun, C.C. Berndt, K.A. Gross, A. Cucuk, Material fundamentals and clinical performance of plasma-sprayed hydroxyapatite coatings: a review, *J. Biomed. Mater. Res.* 58 (2001) 570–592.
- [22] R.B. Heimann, Plasma-sprayed hydroxylapatite-based coatings: chemical, mechanical, microstructural, and biomedical properties, *J. Therm. Spray Technol.* 25 (2016) 827–850.
- [23] P.Y. Chen, S.F. Wang, R.R. Chien, C.S. Tu, K.C. Feng, C.S. Chen, K.Y. Hung, V.H. Schmidt, Evolution of the microstructural and mechanical properties of hydroxyapatite bioceramics with varying sintering temperature, *Ceram. Int.* 45 (2019) 16226–16233.
- [24] S. Suresh, S.W. Lee, M. Aindow, H.D. Brody, V.K. Champagne, A.M. Dongare, Mesoscale modeling of jet initiation behavior and microstructural evolution during

- cold spray single particle impact, *Acta Mater.* 182 (2020) 197–206.
- [25] J. Frattolin, R. Roy, S. Rajagopalan, M. Walsh, S. Yue, O.F. Bertrand, R. Mongrain, A manufacturing and annealing protocol to develop a cold-sprayed Fe-316L stainless steel biodegradable stenting material, *Acta Biomater.* 99 (2019) 479–494.
- [26] Y. Liu, Z. Dang, Y. Wang, J. Huang, H. Li, Hydroxyapatite/graphene-nanosheet composite coatings deposited by vacuum cold spraying for biomedical applications: inherited nanostructures and enhanced properties, *Carbon* 67 (2014) 250–259.
- [27] J.G. Lee, D.Y. Kim, J.H. Lee, M. Kim, S. An, H.S. Jo, C. Nervi, S.S. Al-Deyab, M.T. Swihart, S.S. Yoon, Scalable binder-free supersonic cold spraying of nano-textured cupric oxide (CuO) films as efficient photocathodes, *ACS Appl. Mater. Interfaces* 8 (2016) 15406–15414.
- [28] J. Guillem-Marti, N. Cinca, M. Punset, I.G. Cano, F.J. Gil, J.M. Guilemany, S. Dosta, Porous titanium-hydroxyapatite composite coating obtained on titanium by cold gas spray with high bond strength for biomedical applications, *Colloids Surf., B* 180 (2019) 245–253.
- [29] J. Tang, Z. Zhao, H. Liu, X. Cui, J. Wang, T. Xiong, A novel bioactive Ta/hydroxyapatite composite coating fabricated by cold spraying, *Mater. Lett.* 250 (2019) 197–201.
- [30] A.C.W. Noorakma, H. Zuhailawati, V. Aishvarya, B.K. Dhindaw, Hydroxyapatite-coated magnesium-based biodegradable alloy: cold spray deposition and simulated body fluid studies, *J. Mater. Eng. Perform.* 22 (2013) 2997–3004.
- [31] D.M. Chun, S.H. Ahn, Deposition mechanism of dry sprayed ceramic particles at room temperature using a nano-particle deposition system, *Acta Mater.* 59 (2011) 2693–2703.
- [32] Y. Liu, Y. Wang, X. Suo, Y. Gong, C. Li, H. Li, Impact-induced bonding and boundary amorphization of TiN ceramic particles during room temperature vacuum cold spray deposition, *Ceram. Int.* 4 (2016) 1640–1647.
- [33] A. Friedmann, A. Hoess, A. Cismak, A. Heilmann, Investigation of cell-substrate interactions by focused ion beam preparation and scanning electron microscopy, *Acta Biomater.* 7 (2011) 2499–2507.
- [34] A. Rigort, J.M. Plitzko, Cryo-focused-ion-beam applications in structural biology, *Arch. Biochem. Biophys.* 581 (2015) 122–130.
- [35] H. Assadi, F. Gärtner, T. Stoltenhoff, H. Kreye, Bonding mechanism in cold gas spraying, *Acta Mater.* 51 (2003) 4379–4394.
- [36] M. Grujicic, C.L. Zhao, W.S. DeRosset, D. Helfritsch, Adiabatic shear instability based mechanism for particles/substrate bonding in the cold-gas dynamic-spray process, *Mater. Des.* 25 (2004) 681–688.
- [37] X.T. Luo, Y.K. Wei, Y. Wang, C.J. Li, Microstructure and mechanical property of Ti and Ti₆Al₄V prepared by an in-situ shot peening assisted cold spraying, *Mater. Des.* 85 (2015) 527–533.
- [38] H.P. Felgueiras, M.D.M. Evans, V. Migonney, Contribution of fibronectin and vitronectin to the adhesion and morphology of MC3T3-E1 osteoblastic cells to poly (NaSS) grafted Ti₆Al₄V, *Acta Biomater.* 28 (2015) 225–233.
- [39] D.M. Rivera-Chacon, M. Alvarado-Velez, C.Y. Acevedo-Morantes, S.P. Singh, E. Gultepe, D. Nagesha, S. Sridhar, J.E. Ramirez-Vick, Effect of fibronectin and vitronectin on human fetal osteoblast cell attachment, and proliferation on nanostructured titanium surfaces, *J. Biomed. Nanotechnol.* 9 (2013) 1–6.
- [40] A. Toffoli, L. Parisi, M.G. Bianchi, S. Lumetti, O. Bussolati, G.M. Macaluso, Thermal treatment to increase titanium wettability induces selective proteins adsorption from blood serum thus affecting osteoblasts adhesion, *Mater. Sci. Eng., C* 107 (2020) 110250.
- [41] M.J. Dalby, D. Giannaras, M.O. Riehle, N. Gadegaard, S. Affrossman, A.S. Curtis, Rapid fibroblast adhesion to 27 nm high polymer demixed nano-topography, *Biomaterials* 25 (2004) 77–83.
- [42] J.L. Gallop *Filopodia and their links with membrane traffic and cell adhesion Seminars in Cell & Developmental Biology* 2020 <https://doi-org-443.webvpn.las.ac.cn/10.1016/j.semdb.2019.11.017>.
- [43] M. Motskin, D.M. Wrigh, K. Muller, N. Kyle, T.G. Gard, A.E. Porter, J.N. Skepper, Hydroxyapatite nano and microparticles: correlation of particle properties with cytotoxicity and biostability, *Biomaterials* 30 (2009) 3307–3317.
- [44] S. Pujari-Palmer, S. Chen, S. Rubino, H. Weng, W. Xia, H. Engqvist, L. Tang, M.K. Ott, In vivo and in vitro evaluation of hydroxyapatite nanoparticle morphology on the acute inflammatory response, *Biomaterials* 90 (2016) 1–11.
- [45] C. Chen, Y. Xie, R. Huang, S. Deng, Z. Ren, H. Liao, On the role of oxide film's cleaning effect into the metallurgical bonding during cold spray, *Mater. Lett.* 210 (2018) 199–202.
- [46] X. Zhao, S.X. Ng, B.C. Heng, J. Guo, L.L. Ma, T.T.Y. Tan, K.W. Ng, S.C.J. Loo, Cytotoxicity of hydroxyapatite nanoparticles is shape and cell dependent, *Arch. Toxicol.* 87 (2013) 1037–1052.
- [47] C.H. Kwong, W.B. Burns, H.S. Cheung, Solubilization of hydroxyapatite crystals by murine bone cells, macrophages and fibroblasts, *Biomaterials* 10 (1989) 579–584.
- [48] M.T. Fulmer, I.C. Ison, C.R. Hankermayer, B.R. Constantz, J. Ross, Measurements of the solubilities and dissolution rates of several hydroxyapatites, *Biomaterials* 23 (2002) 751–755.
- [49] S. Ferraris, S. Yamaguchi, N. Barbani, M. Cazzola, C. Cristallini, M. Miola, E. Vernè, S. Spriano, Bioactive materials: In vitro investigation of different mechanisms of hydroxyapatite precipitation, *Acta Biomater.* 102 (2020) 468–480.
- [50] A.E. Porter, L.W. Hobbs, V.B. Rosena, M. Spector, The ultrastructure of the plasma-sprayed hydroxyapatite-bone interface predisposing to bone bonding, *Biomaterials* 23 (2002) 725–733.
- [51] H.C. Blair, Q.C. Larrouture, Y. Li, H. Lin, D. Beer-Stoltz, L. Liu, R.S. Tuan, L.J. Robinson, P.H. Schlesinger, D.J. Nelson, Osteoblast differentiation and bone matrix formation in vivo and in vitro, *Tissue Eng. Part B: Rev.* 23 (2017) 1–29.
- [52] H.C. Anderson, Matrix vesicles and calcification, *Curr. Rheumatol. Rep.* 5 (2003) 222–226.